

# Adaptive Precision Training (ADEPT): A dynamic fixed point quantized sparsifying training approach for DNNs

Lorenz Kummer<sup>12</sup>   Kevin Sidak<sup>13</sup>   Tabea Reichmann<sup>14</sup>   Wilfried Gansterer<sup>15</sup>

August 2021

## Abstract

Quantization is a technique for reducing deep neural networks (DNNs) training and inference times, which is crucial for training in resource constrained environments or time critical inference applications. State-of-the-art (SOTA) approaches focus on post-training quantization, i.e. quantization of pre-trained DNNs for speeding up inference. Little work on quantized training exists and usually, existing approaches require full precision refinement afterwards or enforce a global word length across the whole DNN. This leads to suboptimal bitwidth-to-layers assignments and resource usage. Recognizing these limits, we introduce ADEPT, a new quantized sparsifying training strategy using information theory-based intra-epoch precision switching to find on a *per-layer* basis the lowest precision that causes no quantization-induced information loss while keeping precision high enough for future learning steps to not suffer from vanishing gradients, producing a fully quantized DNN. Based on a bitwidth-weighted MAdds performance model, our approach achieves an average speedup of 1.26 and model size reduction of 0.53 compared to standard training in float32 with an average accuracy increase of 0.98% on AlexNet/ResNet on CIFAR10/100.

## 1 Introduction

With the general trend in machine learning leaning towards large model sizes to solve increasingly complex problems, these models can be difficult to tackle in the context of inference in time critical applications or training under resource and/or productivity constraints. Some applications, where a more time- and space efficient model is crucial, include robotics, augmented reality, self driving vehicles, mobile applications, applications running on consumer hardware or research, needing a high number of trained models for hyper parameter optimization. Accompanied by this, DNN architectures, already some of the most common ones, like AlexNet [1] or ResNet [2], suffer from over-parameterization and overfitting.

Possible solutions to the aforementioned problems include pruning [3, 4, 5, 6, 7, 8], or quantization. When quantizing, the bitwidth of the parameters is decreased, therefore utilizing a lower precision for more efficient use of computing resources, such as memory and runtime. However, quantization has to be performed with a certain caution, as naive approaches or a too low bitwidth can have a negative impact on the accuracy of the network, unacceptable for most use cases. E.g. Binary Quantization [9] can effectively speed up computation, as multiplication can be performed as bit shifts, and further reduce memory, but the accuracy suffers heavily from this approach. Prior approaches mainly quantize the network for inference, or use a global bitwidth, which does not take

<sup>1</sup>Faculty of Computer Science, University of Vienna

<sup>2</sup>lorenz.kummer@univie.ac.at

<sup>3</sup>kevin.sidak@univie.ac.at

<sup>4</sup>tabea.reichmann@univie.ac.at

<sup>5</sup>wilfried.gansterer@univie.ac.at

the differences quantization can have on different layers into account, nor use a dynamic precision switching mechanism based on information theory.

ADEPT extends these approaches and introduces a new precision switching mechanism by applying the Kullback-Leibler-Divergence [10], that calculates the average number of bits lost due to a precision switch. This is done not only for the whole network, but on a per-layer basis, therefore considering differences of effect of quantization on the different layers, leading to **ADaptiveE Precision Training** of DNNs over time during training. Further, our approach does not need full precision refinement, leading to an already quantized network that can then also be deployed on mobile hardware.

## 1.1 Related Work

In general studies of the sensitivity of DNNs, perturbation analysis [11] has been applied to examine historical neural network architectures [12, 13, 14] but also yielded results for the sensitivity of simple modern architectures recently [15].

For exploring the accuracy degradation induced by quantizations of weights, activations and gradients, [16] and [17] introduced the frameworks TensorQuant and QPyTorch, capable of simulating the most common quantizations for training and inference tasks on a float32 basis. Both frameworks allow to freely choose exponent and mantissa for floating-point, word and fractional bit length for fixed-point and word length for block-floating-point representations as well as signed/unsigned representations. Since the quantizations are simulations, no actual speedup can be achieved using these frameworks.

Minimizing inference accuracy degradation, induced by quantizing weights and activations, while leveraging associated performance increases can be achieved by incorporating (simulated) quantization into model training and training the model itself to compensate the introduced errors (Quantization Aware Training, QAT) [18, 19], by learning optimal quantization schemes through jointly training DNNs

and associated quantizers (Learned Quantization Nets, LQ-Nets) [20] or by using dedicated quantization friendly operations [21]. A notably different approach is taken by Variational Network Quantization (VNQ) [22] which uses variational Dropout training [23] with a structured sparsity inducing prior [24] to formulate post-training quantization as the variational inference problem searching the posterior optimizing the Kullback-Leibler-Divergence (KLD) [10]. Machine learning frameworks such as PyTorch or Tensorflow already provide builtin quantization capabilities. These quantization methods focus on either QAT or post-training quantization [25] [26]. Both of these methods only quantize the model after the training and in that provide no speedup during training. Additional processing steps during or after training are needed which add an computational overhead.

From a theoretical viewpoint, quantized training has been investigated by [27] with a particular focus on rounding methods and convergence guarantees. For training on multi-node environments (i.e. distributed), Quantized Stochastic Gradient Descent (QSGD) introduced by [28] incorporates a family of gradient compression schemes aimed at reducing inter-node communication costs occurring during SGD’s gradient updates, producing a significant speedup as well as convergence guarantees under standard assumptions (not included here for brevity, see [29] for details). For speeding up training on a single node via block-floating point quantization, [30] introduced a dynamic training quantization scheme (Multi Precision Policy Enforced Training, MuPPET) that after quantized training outputs a model for float32 inference.

## 1.2 Contributions

We found the SOTA in quantized training and inference solutions leaves room for improvements in several areas. QAT, LQ-Nets and VNQ are capable of producing networks s.t. inference can be executed under quantization with minimal DNN degradation, but require computationally expensive float32 training. MuPPET requires at least  $N$  epochs for

$N$  quantization levels because precision switches are only triggered at the end of an epoch and going through all precision levels is required by the algorithm. Word length is global across the network such that potential advantages coming from different layers of the network storing different amounts of information are negated. The precision switching criterion is only based on the diversity of the gradients of the last  $k$  epochs, no metric is used to measure the actual amount of information lost by applying a certain quantization level to a weights tensor. Precision levels can only increase during training and never decrease. Furthermore, the network produced by MuPPET can only be used for float32 inference. We advance the SOTA by providing an easy-to-use solution for quantized training of DNNs by using an information-theoretical intra-epoch precision switching mechanism capable of dynamically increasing and decreasing the precision of the network on a per-layer basis, resulting in a network for inference that benefits in terms of runtime and model size from being quantized to the lowest precision possible for each layer. Besides its intrinsic methodological advantages, we demonstrate ADEPT is competitive in accuracy degradation and superior in runtime, training AlexNet and ResNet20 on the CIFAR10/100 datasets.

## 2 Background

### 2.1 Quantization

Numerical representation describes how numbers are stored in memory (illustrated by fig. 1) and how arithmetic operations on those numbers are conducted. Commonly available on consumer hardware are floating-point and integer representations while fixed-point or block-floating-point representations are used in high-performance application-specific integrated circuits (ASICs) or field-programmable gate arrays (FPGAs). The numerical precision used by a given numerical representation refers to the amounts of bits allocated for the representation of a single number, e.g. a real number stored in float32 refers to floating-point representation in 32-bit preci-

sion. With these definitions of numerical representation and precision in mind, most generally speaking, quantization is the concept of running a computation or parts of a computation at reduced numerical precision or a different numerical representation with the intent of reducing computational costs and memory consumption. Quantized execution of a computation however can lead to the introduction of an error either through the quantized representations the machine epsilon  $\epsilon_{mach}$  being too large (underflow) to accurately depict resulting real values or the representable range being too small to store the result (overflow).

**Floating-Point Quantization** The value  $v$  of a floating point number is given by  $v = \frac{s}{b^{p-1}} \times b^e$  where  $s$  is the significand (mantissa),  $p$  is the precision (number of digits in  $s$ ),  $b$  is the base and  $e$  is the exponent [31]. Hence quantizing using floating-point representation can be achieved by reducing the number of bits available for mantissa and exponent, e.g. switching from a float32 to a float16 representation, and is offered out of the box by common machine learning frameworks for post-training quantization and quantized training [32, 33].

**Integer Quantization** Integer representation is available for post-training quantization and QAT (int8, int16 due to availability on consumer hardware) in common machine learning frameworks [32, 33]. Quantized training however is not supported by these frameworks due to integer functions not being differentiable.

**Block-Floating-Point Quantization** Block-floating-point represents each number as a pair of  $WL$  (word length) bit signed integer  $x$  and a scale factor  $s$  s.t. the value  $v$  is represented as  $v = x \times b^{-s}$  with base  $b = 2$  or  $b = 10$ . The scaling factor  $s$  is shared across multiple variables (blocks), hence the name block-floating point, and is typically determined s.t. the modulus of the largest element is  $\in [\frac{1}{b}, 1]$  [34]. Block-floating-point arithmetic is used in cases where variables cannot be expressed with sufficient accuracy on native fixed-point hardware.

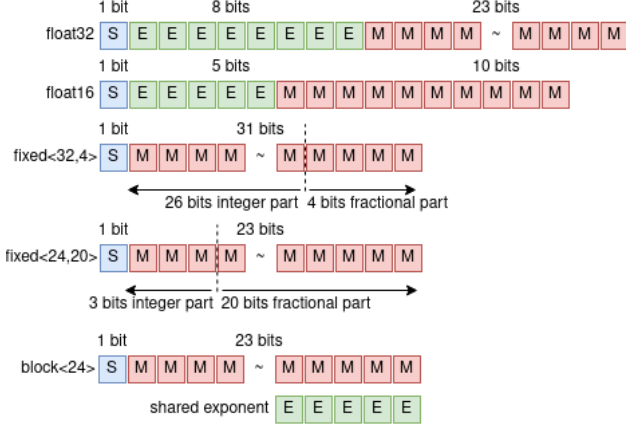


Figure 1: *Examples of floating-point, fixed-point and block-floating-point representations at different numerical precisions*

**Fixed-Point Quantization** Fixed-point numbers have a fixed number of decimal digits assigned and hence every computation must be framed s.t. the results lies within the given boundaries of the representation [35]. By definition of [36], a signed fixed-point numbers of word length  $WL = i + s + 1$  can be represented by a 3-tuple  $\langle s, i, p \rangle$  where  $s$  denotes whether the number is signed,  $i$  denotes the number of integer bits and  $p$  denotes the number of fractional bits.

ADEPT uses fixed-point quantization because unlike block floating point as used by MuPPET with a global word length across the whole network and per-layer shared exponent, we conjecture that optimal word and fractional lengths are local properties of each layer under the hypothesis that different layers contain different amounts of information during different points of time in training. We decided against using floating-point quantization because fixed-point gives us better control over numerical precision and is available in high performance ASICs which are our target platform and against integer quantization due the fact that gradients cannot be computed for integer quantized networks. In principle however, the ADEPT concept could be

extended to representations other than fixed-point.

## 2.2 MuPPET

MuPPET is a mixed-precision DNN training algorithm that combines the use of block-floating and floating-point representations. The algorithm stores two copies of the networks weights: a float32 master copy of the weights that is updated during backwards passes and a quantized copy used for forward passes. MuPPETs uses block-floating point representation as outlined in sec. 2.1 with base  $b = 2$  for quantization. The precision level  $i$  of a layer  $l$  of all layers  $\mathbb{L}$  is defined as  $q_l^i = \langle q_l^i | \forall l \in [1, |\mathbb{L}|] \rangle^i$ :

$$q_l^i = \langle WL^{net}, s_l^{weights}, s_l^{act} \rangle^i$$

with  $WL^{net}$  being global across the network, and scaling factor  $s$  (for weights and activation functions) varying per layer, determined each time precision switch is triggered. The scaling factor for a matrix  $X$  is given by

$$s_{weights,act} = \left\lceil \log_2 \min \left( \left( \frac{UB + 0.5}{\mathbf{X}_{max}^{weights,act}}, \frac{LB - 0.5}{\mathbf{X}_{min}^{weights,act}} \right) \right) \right\rceil$$

with  $\mathbf{X}_{max,min}^{weights,act}$  describing the maximum or minimum value in the weights or feature maps matrix of the layer.  $UB$  and  $LB$  describe the upper bounds and lower bounds of the of the word length  $WL^{net}$ . Its individual elements  $x$  are quantized:

$$x_{quant}^{\{weights,act\}} = \lfloor x^{\{weights,act\}} * 2^{s^{\{weights,act\}}} + \text{Unif}(-0.5, 0.5) \rfloor$$

$\text{Unif}(a, b)$  is the sampling from a uniform distribution in the interval  $[a, b]$ . The parameters 0.5 and  $-0.5$  to add to the bounds is chosen for maximum utilisation of  $WL^{net}$ . During training the precision of the quantized weights is increased using a precision-switching heuristic based on gradient diversity [37], where the gradient of the last mini-batch  $\nabla f_l^j(\mathbf{w})$  of each layer  $l \in \mathbb{L}$  at epoch  $j$  is stored and after a certain number of epochs ( $r$ ), the inter-epoch gradient

diversity  $\Delta s$  at epoch  $j$  is computed by:

$$\Delta s(\mathbf{w})^j = \frac{\sum_{\forall l \in \mathbb{L}} \frac{\sum_{k=j-r}^j \|\nabla f_l^k(\mathbf{w})\|_2^2}{\sum_{k=j-r}^j \|\nabla f_l^k(\mathbf{w})\|_2^2}}{\mathbb{L}}$$

At epoch  $j$  there exists a set of gradient diversities  $S(j) = \{\Delta s(\mathbf{w})^i \mid \forall e \leq i < j\}$  ( $e$  denotes the epoch in which it was switched into the quantization scheme) of which the ratio  $p = \frac{\max S(j)}{\Delta s(\mathbf{w})^i}$  is calculated. If  $p$  violates a threshold for a certain number of times, a precision switch is triggered. Speedups claimed by MuPPET are based on an estimated performance model simulating fixed-point arithmetic using NVIDIA CUTLASS [38] for compatibility with GPUs, only supporting floating and integer arithmetic.

## 3 ADEPT

### 3.1 Quantization Friendly Initialization

Despite exhaustive literature research and to our best knowledge, it has not yet been explored how quantized training impacts vanishing/exploding gradients counter-strategies and vice versa. However the preliminary experimental results of our first investigation of the impact of different weights initialization strategies showed the resilience of DNNs trained under a fixed forwards pass integer quantization scheme (int2, int4, int8, int16) with float32 master copies for gradient computations correlates strongly with initializer choice (fig. 2). Using Adam [39] as optimizer, we trained LeNet-5 [40] on MNIST/FMNIST [41] and AlexNet on CIFAR10/100 [42] and examined the degree to which the quantized networks are inferior in accuracy compared to baseline networks trained in float32 dependent on initializer choice (Random Normal, Truncated Normal, Random Uniform, Glorot Normal/Uniform [43], He Normal/Uniform [44], Variance Scaling [45], Lecun Normal/Uniform [46, 47]) and initializer parameters. We found that DNNs initialized by fan-in truncated normal variance scaling (TNVS) degrade least under quantized training with a fixed integer quantization scheme as described

above. This correlates with results published by [48] who introduced a learnable scale parameters in their asymmetric quantization scheme to achieve more stable training. We thus initialize networks with TNVS and an empirically chosen scaling factor  $s$  where  $n_i$  is the number of input units of a weights tensor  $W_i$  before quantized training with ADEPT.

$$W_i \sim N\left(\sigma = \sqrt{\frac{s}{n_i}}, \mu = 0, \alpha = \pm \sqrt{\frac{3 \cdot s}{n_i}}\right)$$

The examination of how other counter strategies (eg. gradient amplification, [49], gradient normalization [50], weights normalization [51]) affect quantized training remains an open question.

### 3.2 Precision Levels

ADEPT uses signed fixed-point representation as defined in sec. 2.1 and stochastic rounding, which in combination with a fixed-point representation has been shown to consistently outperform nearest-rounding by [36], for quantizing float32 numbers. Given that ADEPT is agnostic towards whether a number is signed or not, we represent the precision level of each  $l \in \mathbb{L}$  simply as  $\langle WL^l, FL^l \rangle$  whereby fractional length  $FL^l$  denotes the number of fractional bits. For a random number  $P \in [0, 1]$ ,  $x$  is stochastically rounded by

$$SR(x) = \begin{cases} \lfloor x \rfloor, & \text{if } P \geq \frac{x - \lfloor x \rfloor}{\epsilon_{mach}} \\ \lfloor x \rfloor + 1, & \text{if } P < \frac{x - \lfloor x \rfloor}{\epsilon_{mach}} \end{cases}$$

### 3.3 Precision Switching Mechanism

Precision switching in quantized DNN training is the task of carefully balancing the need to keep precision as low as possible in order to improve runtime and model size, yet still keep enough precision for the network to keep learning. In ADEPT, we have encoded these opposing interests in two operations, the PushDown Operation and the PushUp Operation.

**The PushDown Operation** Determining the amount of information lost if the precision of the fixed-point representation of a layer's weight tensor is

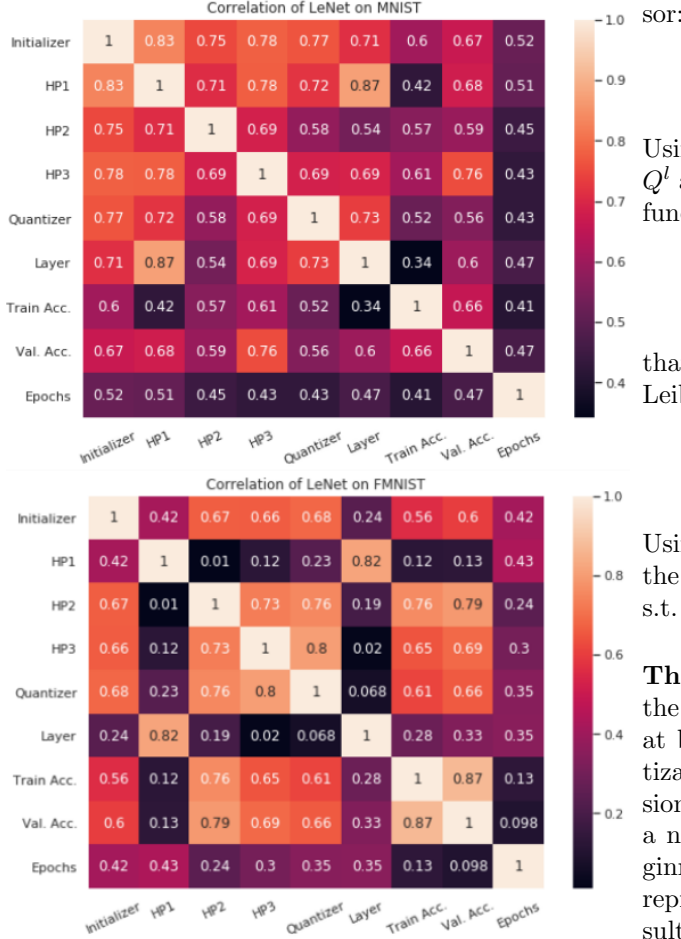


Figure 2: Correlation of initializer choice, hyperparameters (HP), quantizer, layer, training and validation accuracy, duration of training (epochs) for LeNet5 on MNIST and FMNIST datasets

lowered, can be heuristically accomplished by interpreting the precision switch as a change of encoding. Assume a weights tensor  $\mathbf{W}^l \sim Q$  of layer  $l \in \mathbb{L}$  with its quantized counterpart  $\widehat{\mathbf{W}}^l \sim P^l$ , where  $P^l, Q^l$  are the respective distributions. Then the continuous Kullback-Leibler-Divergence [10] (1) represents the average number of bits lost through changing the encoding of  $l$  from  $Q^l$  to  $P^l$ , with  $p$  and  $q$  denoting probabilities, and  $w$  the elements of the weights ten-

SOR:

$$D(P^l \| Q^l) = \int_{-\infty}^{\infty} p^l(w) \cdot \log \frac{p^l(w)}{q^l(w)} dw$$

Using discretization via binning, we obtain  $P^l$  and  $Q^l$  at resolution  $r^l$  through the empirical distribution function:

$$\widehat{F}_{r^l}^l(w) = \frac{1}{r^l + 1} \sum_{i=1}^{r^l} 1_{W_i^l \leq w} \quad (1)$$

that can then be used in the discrete Kullback-Leibler-Divergence (2).

$$KL(P^l \| Q^l) = \sum_{w \in \mathbf{W}^l} P^l(w) \cdot \log \frac{P^l(w)}{Q^l(w)} \quad (2)$$

Using a bisection approach, ADEPT efficiently finds the smallest quantization  $\langle WL_{min}^l, FL_{min}^l \rangle$  of  $\mathbf{W}^l$  s.t.  $KL(P^l \| Q^l) > 0 \forall l \in \mathbb{L}$

**The PushUp Operation** However, determining the precision of the fixed-point representation of  $\mathbf{W}^l$  at batch  $j$ , s.t. the information lost through quantization is minimal but there is still sufficient precision for subsequent batches  $j+1$  to keep learning, is a non-trivial task. Solely quantizing  $\mathbf{W}^l$  at the beginning of the training to a low precision fixed-point representation (e.g.  $\langle WL^l, FL^l \rangle = \langle 8, 4 \rangle$ ) would result in the network failing to learn, because at such low precision levels, gradients would vanish very early on in the backwards pass. Hence, ADEPT tracks for each layer a second heuristic over the last  $j$  batches to determine how much precision is required for the network to keep learning. If gradients are quantized, a gradient diversity based heuristic is employed (3), (5).

$$\Delta s(\mathbf{w})_j^l = \frac{\sum_{k=j-r}^j \|\nabla f_k^l(\mathbf{w})\|_2}{\|\sum_{k=j-r}^j \nabla f_k^l(\mathbf{w})\|_2} \quad (3)$$

$$\Delta \tilde{s}(\mathbf{w})_j^l = \begin{cases} \log \Delta s(\mathbf{w})_j^l & \text{if } 0 < \Delta s(\mathbf{w})_j^l < \infty \\ 1 & \text{otherwise} \end{cases}$$

If  $\Delta \tilde{s}(\mathbf{w})_j^l > 0$ , two suggestions for an increase in precision are computed,  $s_1^l = \max(\lceil \frac{1}{\log \Delta s(\mathbf{w})_j^l - 1} \rceil, 1)$  and

$s_2^l = \max(\min(32 \cdot \log^2 \Delta s(\mathbf{w})_j^l - 1, 32) - FL_{min}^l, 1)$  and the final suggestion is computed dependent on a global strategy  $st$  via

$$s^l = \begin{cases} \min(s_1^l, s_2^l) & \text{if } st = \text{min} \\ \lceil 0.5 \cdot (s_1^l + s_2^l) \rceil & \text{if } st = \text{mean} \\ \max(s_1^l, s_2^l) & \text{if } st = \text{max} \end{cases} \quad (4)$$

Otherwise, i.e.  $\Delta \tilde{s}(\mathbf{w})_j^l > 0$ ,  $s^l = 1$ . The new fixed-point quantization of layer  $l$  is then obtained by  $FL^l = (\min(FL_{min}^l + s^l, 32))$ ,  $WL^l = \min(\max(WL_{min}^l, FL_{min}^l) + 1, 32)$ .

**Dealing with Fixed-Points Limited Range** As outlined in sec. 2.1, fixed-point computations must be framed s.t. results fit within the given boundaries. We approach this by adding a number of buffer bits  $buff$  to every layers word-length, i.e. at the end of PushUp,  $FL^l = (\min(FL_{min}^l, 32 - buff))$ ,  $WL^l = \max(\min(FL_{min}^l + buff, 32), WL_{min}^l)$ . Additionally, we normalize gradients to limit weight growth and reduce chances of weights becoming unrepresentable in the given precision after an update step.

$$\nabla f^l(\mathbf{w}) = \frac{\nabla f^l(\mathbf{w})}{\|\nabla f^l(\mathbf{w})\|_2}$$

**Strategy, Resolution and Lookback** For adapting the strategy  $st$  mentioned in (4), we employ a simple loss-based heuristic. First we compute the average lookback over all layers  $lb_{avg} = |\mathbb{L}|^{-1} \sum_{i=0}^{|\mathbb{L}|} lb^i$  and average loss  $\mathcal{L}_{avg} = |\mathcal{L}|^{-1} \sum_{i=0}^{lb_{avg}} \mathcal{L}_i$  over the last  $lb_{avg}$  batches. Then via (5), the strategy is adapted.

$$st = \begin{cases} \max & \text{if } |\mathcal{L}_{avg}| \leq |\mathcal{L}_i| \text{ and } st = \text{'mean'}$$

$$\begin{cases} \text{mean} & \text{if } |\mathcal{L}_{avg}| \leq |\mathcal{L}_i| \text{ and } st = \text{'min'}$$

$$\begin{cases} \min & \text{if } |\mathcal{L}_{avg}| > |\mathcal{L}_j| \end{cases}$$

Because the number of gradients collected for each layer affects the result of the gradient diversity based heuristic (3), (5), we introduce a parameter lookback  $lb^l$  bounded by hyperparameters

$lb_{lwr} \leq lb^l \leq lb_{upr}$  which is estimated at runtime. First,  $lb_{new}$  is computed:

$$lb_{new}^l = \begin{cases} \min(\max(\lceil \frac{lb_{upr}}{\Delta s(\mathbf{w})_j^l} \rceil, lb_{lwr}), lb_{upr}) & \text{if } 0 < \Delta s(\mathbf{w})_j^l \\ lb_{upr} & \text{otherwise} \end{cases}$$

Then, to prevent jitter, a simple momentum is applied to obtain the updated  $lb^l = \lceil lb_{new}^l \cdot \gamma + (1 - \gamma) \cdot lb^l \rceil$  with  $\gamma \in [0, 1]$ .

Similarly, the number of bins used in the discretization step (1) affects the result of the discrete Kullback-Leibler-Divergence (2). We control the number of bins via a parameter referred to as resolution  $r^l$ , which is derived at runtime and bounded by hyperparameters  $r_{lwr} \leq r^l \leq r_{upr}$ .

$$r^l = \begin{cases} \min(\max(r^l + 1, r_{lwr}), r_{upr}) & \text{if } lb^l = lb_{upr} \\ \min(\max(r^l - 1, r_{lwr}), r_{upr}) & \text{if } lb^l = lb_{lwr} \end{cases} \quad (5)$$

### 3.4 ADEPT-SGD (ASGD)

Although ADEPT can in principle be combined with any iterative gradient based optimizer (e.g. Adam), we chose to implement ADEPT with Stochastic Gradient Descent (SGD), because it generalizes better than adaptive gradient algorithms [52]. The implementation of ADEPT employs the precision switching mechanism and numeric representation described in sec. 3, by splitting it in two operations: the PushDown Operation (alg. 3), which, for a given layer, finds the smallest fixed-point representation that causes no information loss, and the PushUp Operation (alg. 4), which, for a given layer, seeks the precision that is required for the network to keep learning. The integration of these two operations into the precision switching mechanism is depicted in alg. 2, and the integration into SGD training process is depicted in alg. 1.

**Inducing Sparsity** In addition to the ADEPT precision switching mechanism, we used an L1 sparsifying regularizer [53, 54, 55] to obtain sparse and particularly quantization-friendly weight tensors, com-

bined linearly with L2 regularization for better accuracy in a similar way as proposed by [56], thus loss in ASGD is computed by:

$$\hat{\mathcal{L}}(W) = \alpha \|W\|_1 + \frac{\beta}{2} \|W\|_2^2 + \mathcal{L}$$

**Data:** Untrained Float32 DNN  
**Result:** Trained and Quantized DNN

```

1  $\hat{\mathbb{L}} = \text{InitFixedPointTNVS}()$ 
2  $\mathbb{Q} = \text{InitQuantizationMapping}(\hat{\mathbb{L}})$ 
3  $\mathbb{L} = \text{Float32Copy}(\hat{\mathbb{L}})$ 
4 for Epoch in Epochs do
5   for Batch in Batches do
6      $\hat{\mathbb{G}}, \mathcal{L} = \text{ForwardPass}(\hat{\mathbb{L}}, \text{Batch})$ 
7      $\mathbb{Q} = \text{PrecisionSwitch}(\hat{\mathbb{G}}, \mathcal{L}, \mathbb{Q}, \mathbb{L})$ 
8      $\text{SGDBackwardsPass}(\mathbb{L}, \hat{\mathbb{G}})$ 
9     for  $l \in \mathbb{L}$  do
10       $\hat{\mathbb{L}}[l] = \text{Quantize}(\mathbb{L}[l], \mathbb{Q}[l][\text{quant}])$ 
11    end
12  end
13 end
```

**Algorithm 1:** ADEPT-SGD

**Algorithm** When ADEPT-SGD (alg. 1) is started on an untrained float32 DNN, it first initializes the DNNs weights (denoted as  $\hat{\mathbb{L}}$ ) with TNVS (alg. 1, ln. 1). Next the quantization mapping  $\mathbb{Q}$  is initialized, which assigns each  $l \in \mathbb{L}$  a tuple  $\langle WL^l, FL^l \rangle$ , a lookback  $lb^l$  and a resolution  $r^l$  (alg. 1, ln. 2). Then a float32 master copy  $\mathbb{L}$  of  $\hat{\mathbb{L}}$  is created (alg. 1, ln. 3). During training for each forward pass on a batch, quantized gradients  $\hat{\mathbb{G}}$  and loss  $\mathcal{L}$  are computed with a forward pass using quantized layers  $\hat{\mathbb{L}}$  (alg. 1, ln. 4-6). The precision switching mechanism described in sec. 3 is then called (alg. 1, ln. 7) and after adapting the push up strategy as described in sec. 3, it iterates over  $l \in \mathbb{L}$  (alg. 2 ln. 2), first adapting resolution  $r^l$  and lookback  $lb^l$  (alg. 2 ln. 4-5) and then executing PushDown and PushUp on layer  $l$  (alg. 2 ln. 6-10) to update  $\langle WL^l, FL^l \rangle \in \mathbb{Q}$ . When PushDown is called on  $l$ , it decreases the quantization mapping in a bisectional fashion until  $KL$  indicates a lower quantization would cause information loss at resolution  $r^l$

**Data:**  $\hat{\mathbb{G}}, \mathcal{L}, \mathbb{Q}, \mathbb{L}$   
**Result:**  $\mathbb{Q}$

```

1  $\text{AdaptStrategy}(\mathcal{L})$ 
2 for  $l \in \mathbb{L}$  do
3    $\mathbb{Q}[l][\text{grads}].\text{append}(\hat{\mathbb{G}}[l])$ 
4    $\text{AdaptLookback}(\mathbb{Q}[l][\text{grads}], \mathbb{Q}[l][lb])$ 
5    $\text{AdaptResolution}(\mathbb{Q}[l][lb], \mathbb{Q}[l][res])$ 
6   if  $|\mathbb{Q}[l][\text{grads}]| \geq \mathbb{Q}[l][lb]$  then
7      $WL^l, FL^l = \mathbb{Q}[l][\text{quant}]$ 
8      $WL_{min}^l, FL_{min}^l = \text{PushDown}(\mathbb{L}[l], WL^l, FL^l)$ 
9      $WL_{new}^l, FL_{new}^l = \text{PushUp}(l, WL^l, FL^l, WL_{min}^l, FL_{min}^l)$ 
10     $\mathbb{Q}[l][\text{quant}] = WL_{new}^l, FL_{new}^l$ 
11  end
12 end
```

**Algorithm 2:** PrecisionSwitch

**Data:**  $L, WL^l, FL^l$   
**Result:**  $WL_{min}^l, FL_{min}^l$

```

1  $WL_{min}^l, FL_{min}^l = L, WL^l, FL^l$ 
2 repeat
3    $WL_{min}^l, FL_{min}^l = \text{Decrease}(WL_{min}^l, FL_{min}^l)$ 
4    $\hat{L} = \text{Quantize}(L, WL_{min}^l, FL_{min}^l)$ 
5 until  $KL(EDF(L_i), EDF(\hat{L})) < \epsilon$ 
```

**Algorithm 3:** PushDown Operation

(3, ln. 1-5). After computing the lowest quantization  $\langle WL_{min}^l, FL_{min}^l \rangle \in \mathbb{Q}$  not causing information loss in  $l$ , PushUp is called on  $l$  to increase the quantization to the point where the network is expected to keep learning, based on gradient diversity of the last  $lb^l$  batches (alg. 4, ln. 1-6). After PushUp the PrecisionSwitch returns an updated  $\mathbb{Q}$  to the training loop, and a regular SGD backward pass updates the float32 master copy  $\mathbb{L}$ , using quantized gradients  $\hat{\mathbb{G}}$  (alg. 1, ln. 7,8). Finally, the now updated weights  $\mathbb{L}$  are quantized using the updated  $\mathbb{Q}$  and written back to  $\hat{\mathbb{L}}$  to be using in the next forward pass (alg. 1, ln. 9-11).



**Data:**  $L, WL^l, FL^l, WL_{min}^l, FL_{min}^l$   
**Result:**  $WL_{new}^l, FL_{new}^l$

- 1 Compute  $\widehat{\Delta s}(L)$  using  $WL_{min}^l, FL_{min}^l$
- 2 Compute  $\Delta s(L)$  using  $WL^l, FL^l$
- 3 **while**  $\Delta s(L) \geq \widehat{\Delta s}(L)$  **do**
- 4      $WL_{min}^l, FL_{min}^l = \text{Increase}(WL_{min}^l, FL_{min}^l)$
- 5     Compute  $\widehat{\Delta s}(L)$  using  $WL_{min}^l, FL_{min}^l$
- 6 **end**

**Algorithm 4:** PushUp Operation

## 4 Experimental Evaluation

### 4.1 Setup

For experimental evaluation of ADEPT, we trained AlexNet and ResNet20 on the CIFAR-10/100 datasets with reduce on plateau learning rate (ROP) scheduling which will reduce learning rate by a given factor if loss has not decreased for a given number of epochs [32]. Due to unavailability of fixed-point arithmetic, we used QPyTorch to simulate fixed point arithmetic and our own performance model (sec. 4.1.2) to simulate speedups, model size reductions and memory consumption. Experiments were conducted on a Nvidia DGX-1 sponsored by Visualization and Data Analysis Research Group at University of Vienna. It has 8 x Tesla V100 GPUs, which is capable of integer and floating-point arithmetic [57].

#### 4.1.1 Hyper Parameters

All layers  $l \in \mathbb{L}$  were quantized with  $\langle WL^l, FL^l \rangle = \langle 8, 4 \rangle$  at the beginning of ADEPT training. Other hyperparameters specific to ADEPT were set to  $r_{lwr} = 50$ ,  $r_{upr} = 150$ ,  $lb_{lwr} = 25$ ,  $lb_{upr} = 100$ , look-back momentum  $\gamma = 0.33$  for all experiments, buffer bits was set to  $buff = 4$  for training AlexNet on CIFAR10 and  $buff = 8$  for training ResNet and AlexNet on CIFAR100. Hyperparameters unspecific to ADEPT ( $lr$ ,  $L1_{decay}$ ,  $L2_{decay}$ ,  $ROP_{patience}$ ,  $ROP_{threshold}$  *batch size*, *accumulation steps*) were selected using grid search and 10-fold cross-validation for each the float32 and the quantized networks in-

dependently and we refer to our code repository<sup>1</sup> for the exact configuration files of each experiment.

#### 4.1.2 Performance Model

Speedups and model size reductions were computed using a performance model taking forward and backward passes, as well as batch sizes, gradient accumulations numerical precision and sparsity, into account. Our performance model computes per layer operations (MAdds, subsequently referred to as ops), weights them with the layer’s world length and a tensors percentage of non-zero elements at a specific stage in training to simulate quantization and a sparse tensor format, and aggregates them to obtain the overall incurred computational costs of all forwards and backwards passes. Additionally, the performance model estimates ADEPTs overhead for each layers  $l$  push up operation  $pu^l$  and push down operation  $pd^l$  by

$$ops_{pd,i}^l \leq 2 \cdot \log_2(32 - 8) \cdot r_i^l \cdot 3 \cdot \prod_{dim \in l} dim \quad (6)$$

$$ops_{pu,i}^l \leq (lb_i + 1) \cdot \prod_{dim \in l} dim + 1 \quad (7)$$

Using (6), (7) and the simplifying assumption that a backwards pass incurs as many operations as a quantized forwards pass but is conducted in full precision i.e. 32 bits word length with non-sparse gradients, ADEPTs training costs are then bounded by

$$costs_{train} \leq \sum_{i=1}^n \sum_{l=1}^{|\mathbb{L}|} ops^l \cdot \left( sp_i^l \cdot WL_i^l + \frac{32}{accs} \right) \quad (8)$$

and ADEPTs overhead is bounded by

$$costs_{ADEPT} \leq \sum_{i=1}^n \sum_{l=1}^{|\mathbb{L}|} 32 \cdot \frac{sp_i^l \cdot ops_{pd,i}^l + ops_{pu,i}^l}{accs \cdot lb_i^l} \quad (9)$$

where  $n$  is the number of training steps,  $\mathbb{L}$  are the networks layers and  $WL_i^l$  is the  $l$ -th layers word length at training step  $i$  and  $sp_i^l$  is the percentage of non-zero elements of layer  $l$  at step  $i$ . Using (8), (9), we obtain

<sup>1</sup><https://gitlab.cs.univie.ac.at/sidakk95cs/marvin2>

total costs via  $costs = cost_{train} + costs_{ADEPT}$  and further the speedup of our training approach compared to MuPPET or a float32 baseline incorporating batch size  $bs$ , gradient accumulation steps  $accs$  and computational costs  $costs$  is thus obtained via

$$SU = \frac{bs_{other} \cdot costs_{other}}{bs_{ours} \cdot costs_{ours}}$$

whereby naturally we exclude ADEPTs overhead when computing  $costs_{other}$ . Models size reductions  $SZ$  were calculated by first computing individual model sizes  $sz$

$$sz = \sum_{l=1}^{|\mathbb{L}|} sp_i^l \cdot WL_i^l$$

with  $i = n$  and then forming the quotient  $SZ = sz_{other}/sz_{ours}$ . Similarly, average memory consumption during training  $MEM = mem_{other}/mem_{ours}$  is formed by the quotient of each models memory consumption  $mem$

$$mem = \left( \sum_{i=1}^n \sum_{l=1}^{|\mathbb{L}|} (sp_i^l \cdot WL_i^l + 32) \right) \cdot \frac{1}{n}$$

Because  $sz$  and  $mem$  ignore tensor dimensions, they can not be interpreted as absolute values. However given that in the quotients  $MEM$  and  $SZ$  the effects of tensor dimensions would cancel out when comparing identical architectures (i.e. float32 AlexNet and quantized AlexNet), these values provide valid relative measures for memory consumption and model size under this constraint.

## 4.2 Results

Tab. 1 shows the top-1 validation accuracies and accuracy differences achieved by ADEPT and MuPPET for both quantized training on CIFAR100, and a float32 basis. Tab. 2 shows results for training on CIFAR10. As can be seen in the tables, ADEPT is capable of quantized training to an accuracy comparable to float32 training, and in 100% of the examined cases even surpasses the baseline accuracy. The chosen experiments furthermore illustrate that ADEPT

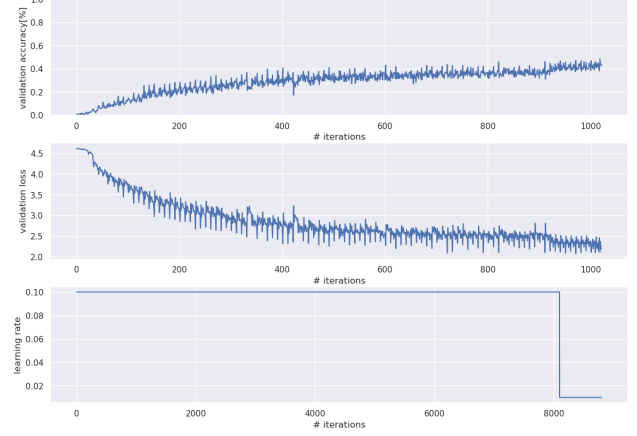


Figure 3: ADEPT learning rate, validation loss, accuracy

CIFAR100				
	Float32	Quantized	$\Delta$	
AlexNet <sub>ADEPT</sub>	41.3 <sup>100</sup> <sub>256</sub>	42.1 <sup>100</sup> <sub>256</sub>	0.8	
AlexNet <sub>MuPPET</sub>	38.2 <sup>150</sup> <sub>128</sub>	38.2 <sup>7</sup> <sub>128</sub>	0.0	
ResNet <sub>ADEPT</sub>	64.3 <sup>100</sup> <sub>256</sub>	65.2 <sup>100</sup> <sub>256</sub>	0.9	
ResNet <sub>MuPPET</sub>	64.6 <sup>150</sup> <sub>128</sub>	65.8 <sup>7</sup> <sub>128</sub>	1.2	

Table 1: Top-1 accuracies, ADEPT (ours) vs MuPPET, CIFAR10, 100 to 150 epochs. Float 32 indicates 32-bit floating-point training (baseline), Quantized indicates variable bit fix-point (ADEPT) or block-floating-point (MuPPET) quantized training, subscript indicates batch size used, superscript indicates epochs used

CIFAR10				
	Float32	Quantized	$\Delta$	
AlexNet <sub>ADEPT</sub>	73.1 <sup>100</sup> <sub>256</sub>	74.1 <sup>150</sup> <sub>256</sub>	1.0	
AlexNet <sub>MuPPET</sub>	75.5 <sup>150</sup> <sub>128</sub>	74.5 <sup>99</sup> <sub>128</sub>	-1.0	
ResNet <sub>ADEPT</sub>	89.0 <sup>100*</sup> <sub>256</sub>	90.2 <sup>100</sup> <sub>256</sub>	1.2	
ResNet <sub>MuPPET</sub>	90.1 <sup>150</sup> <sub>128</sub>	90.9 <sup>114</sup> <sub>128</sub>	0.8	

Table 2: Top-1 accuracies, ADEPT (ours) vs MuPPET, CIFAR100

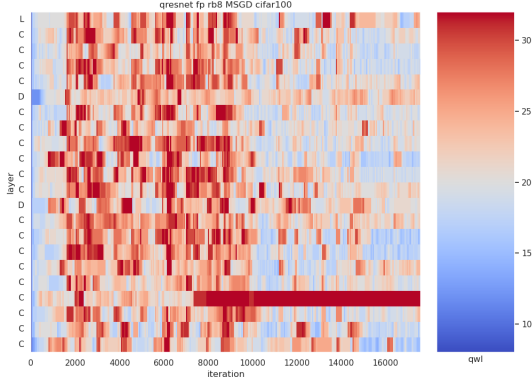


Figure 4: *Wordlengths (bit) of ASGD optimized ResNet20 on CIFAR100*

CIFAR10	MEM	SZ	SU <sup>1</sup>	SU <sup>2</sup>
AlexNet <sub>ADEPT</sub>	1.58	0.65	1.27	4.25
AlexNet <sub>MuPPET</sub>	1.66	1.0	?	1.2
ResNet <sub>ADEPT</sub>	1.76	0.56	1.09	3.13
ResNet <sub>MuPPET</sub>	1.61	1.0	?	1.25

Table 3: Memory Footprint, Final Model Size, Memory Footprint, Speedup, ADEPT (ours) vs MuPPET on respective baseline float32 training on CIFAR10. SU<sup>1</sup>: our baseline, our performance model, SU<sup>2</sup>: MuPPET baseline, our performance model

delivers this performance independent of the underlying DNN architecture or the dataset used. Fig. 4 and 5 display word length usage over time for individual layers for ResNet20 and AlexNet on CIFAR100. In both cases, we observe that individual layers have different precision preferences dependent on progression of the training, an effect that is particularly pronounced in AlexNet. For ResNet20, the word length interestingly decreased notably in the second half of training, which we conjecture is attributable to sparsifying L1 regularization leading to a reduction in irrelevant weights, that would otherwise offset the KL heuristic used in the PushDown Operation. Tabs. 4 and 3 show ADEPTs estimated speedups

CIFAR100	MEM	SZ	SU <sup>1</sup>	SU <sup>2</sup>
AlexNet <sub>ADEPT</sub>	1.35	0.36	1.41	5.54
ResNet <sub>ADEPT</sub>	1.68	0.53	1.13	2.92

Table 4: Memory Footprint, Final Model Size, Memory Footprint, Speedup, ADEPT (ours) vs MuPPET, CIFAR100.

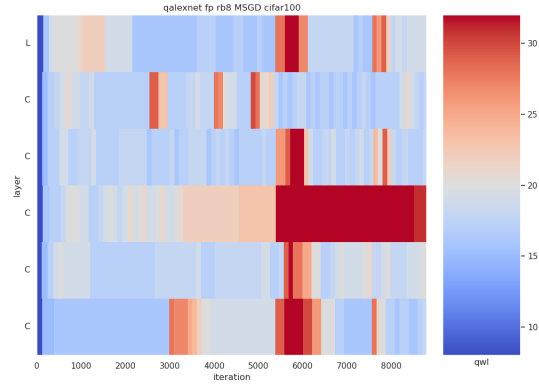


Figure 5: *Wordlengths (bit) of ASGD optimized AlexNet on CIFAR100*

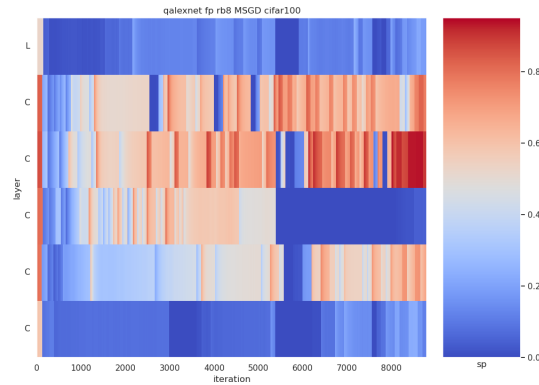


Figure 6: *Sparsity of ASGD optimized ResNet on CIFAR100*

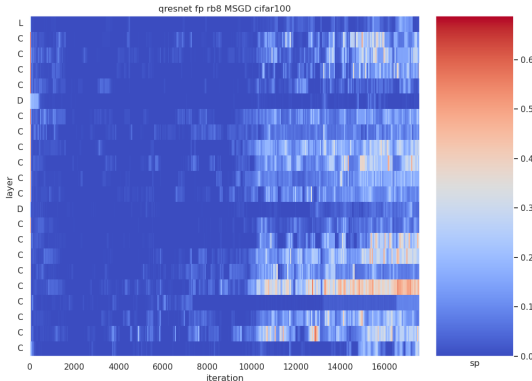


Figure 7: *Sparsity of ASGD optimized ResNet on CIFAR100*

vs. our float32 baseline (100 epochs, same number of gradient accumulation steps and batch size as ADEPT trained models) and MuPPETs float32 baseline. ADEPT achieves speedups comparable with SOTA solutions on our own baseline and outperforms MuPPET on MuPPETs baseline in every scenario. Unfortunately, MuPPET code base could not be executed so we were unable to apply MuPPET to the more efficient ADEPT baseline and were limited to comparing against results provided by the original authors and we used our performance model for simulating MuPPETs performance based on the precision switches stated in the MuPPET paper because MuPPETs authors did not publish their performance model. Fig. 6 and fig. 7 illustrate the induction of sparsity during ADEPT training. Interestingly, we observe an increasing degree of sparsity as ADEPT training progresses, with some layers reaching 80% sparsity and more at the end of training as is the case with AlexNet trained on CIFAR100. As can be seen in tab. 5, ADEPT induces most sparsity in AlexNet, with a 34% final model sparsity and an average intra-training sparsity of 45% for training on CIFAR100. Even in more complex architectures like ResNet we can observe that ADEPT introduces 17% sparsity in the final model. This shows an additional property that reduces the overall runtime and model size with

	<b>Final Model</b>	<b>Average</b>
<b>AlexNet</b> <sub>CIFAR10</sub>	0.19	0.21
<b>ResNet</b> <sub>CIFAR10</sub>	0.14	0.04
<b>AlexNet</b> <sub>CIFAR100</sub>	0.34	0.45
<b>ResNet</b> <sub>CIFAR100</sub>	0.17	0.06

Table 5: Final model sparsity and average intra-training sparsity for ADEPT Training

no compromise regarding accuracy.

## 5 Conclusion

With ADEPT we introduce a novel quantized DNN sparsifying training algorithm that can be combined with any iterative gradient based training scheme. ADEPT exploits fast fixed-point operations for forward passes, while executing backward passes in highly precise float32. By carefully balancing the need to minimize the fixed-point precision for maximum speedup and minimal memory requirements, while at the same time keeping precision high enough for the network to keep learning, our approach produces top-1 accuracies comparable or better than SOTA float32 techniques or other quantized training algorithms. Furthermore ADEPT has the intrinsic methodical advantage of not only training the network in a quantized fashion, but also the trained network itself is quantized and sparsified s.t. it can be deployed to fast ASIC hardware at reduced memory cost compared to a full precision model. Additionally we contribute a performance model for fixed point quantized training.

## 6 Future Work

ADEPT as presented employs a fixed-point representation to enable fine granular precision switches. However, fixed-point hardware is not as common as floating-point hardware, so we plan to extend the concept to floating point quantization s.t. ADEPT becomes compatible with float16/float32 consumer hardware. Additionally, we conjecture the heuristics

used by ADEPT can be used for intra-training DNN pruning as well, which will be subject to future research.

## References

- [1] A. Krizhevsky, I. Sutskever, and G. E. Hinton, “Imagenet classification with deep convolutional neural networks,” in *Advances in neural information processing systems*, pp. 1097–1105, 2012.
- [2] K. He, X. Zhang, S. Ren, and J. Sun, “Deep residual learning for image recognition,” in *Proceedings of the IEEE conference on computer vision and pattern recognition*, pp. 770–778, 2016.
- [3] A. Gordon, E. Eban, O. Nachum, B. Chen, H. Wu, T.-J. Yang, and E. Choi, “Morphnet: Fast & simple resource-constrained structure learning of deep networks,” in *Proceedings of the IEEE conference on computer vision and pattern recognition*, pp. 1586–1595, 2018.
- [4] F. N. Iandola, S. Han, M. W. Moskewicz, K. Ashraf, W. J. Dally, and K. Keutzer, “Squeezenet: Alexnet-level accuracy with 50x fewer parameters and 0.5 mb model size,” *arXiv preprint arXiv:1602.07360*, 2016.
- [5] S. Han, H. Mao, and W. J. Dally, “Deep compression: Compressing deep neural network with pruning, trained quantization and huffman coding,” in *4th International Conference on Learning Representations, ICLR 2016, San Juan, Puerto Rico, May 2-4, 2016, Conference Track Proceedings* (Y. Bengio and Y. LeCun, eds.), 2016.
- [6] J. Fang, Y. Sun, Q. Zhang, K. Peng, Y. Li, W. Liu, and X. Wang, “Fna++: Fast network adaptation via parameter remapping and architecture search,” *IEEE Transactions on Pattern Analysis and Machine Intelligence*, pp. 1–1, 2020.
- [7] W. Hua, Y. Zhou, C. M. De Sa, Z. Zhang, and G. E. Suh, “Channel gating neural networks,” in *Advances in Neural Information Processing Systems* (H. Wallach, H. Larochelle, A. Beygelzimer, F. d’Alché-Buc, E. Fox, and R. Garnett, eds.), vol. 32, Curran Associates, Inc., 2019.
- [8] M. Lis, M. Golub, and G. Lemieux, “Full deep neural network training on a pruned weight budget,” in *Proceedings of Machine Learning and Systems* (A. Talwalkar, V. Smith, and M. Zaharia, eds.), vol. 1, pp. 252–263, 2019.
- [9] M. Courbariaux, I. Hubara, D. Soudry, R. El-Yaniv, and Y. Bengio, “Binarized neural networks: Training deep neural networks with weights and activations constrained to +1 or -1,” 02 2016.
- [10] S. Kullback and R. A. Leibler, “On information and sufficiency,” *The annals of mathematical statistics*, vol. 22, no. 1, pp. 79–86, 1951.
- [11] N. J. Higham, *Accuracy and Stability of Numerical Algorithms*, ch. 7, pp. 119–137.
- [12] K. Wang and A. N. Michel, “Robustness and perturbation analysis of a class of artificial neural networks,” *Neural Networks*, vol. 7, no. 2, pp. 251–259, 1994.
- [13] A. Meyer-Baese, “Perturbation analysis of a class of neural networks,” in *Proceedings of International Conference on Neural Networks (ICNN’97)*, vol. 2, pp. 825–828 vol.2, 1997.
- [14] Xiaoqin Zeng and D. S. Yeung, “Sensitivity analysis of multilayer perceptron to input and weight perturbations,” *IEEE Transactions on Neural Networks*, vol. 12, no. 6, pp. 1358–1366, 2001.
- [15] L. Xiang, X. Zeng, Y. Niu, and Y. Liu, “Study of sensitivity to weight perturbation for convolution neural network,” *IEEE Access*, vol. 7, pp. 93898–93908, 2019.
- [16] D. M. Lorocho, F.-J. Pfreundt, N. Wehn, and J. Keuper, “Tensorquant: A simulation toolbox for deep neural network quantization,” in *Proceedings of the Machine Learning on HPC Environments*, pp. 1–8, 2017.

- [17] T. Zhang, Z. Lin, G. Yang, and C. De Sa, “Qpytorch: A low-precision arithmetic simulation framework,” *arXiv preprint arXiv:1910.04540*, 2019. <https://arxiv.org/pdf/1910.04540.pdf>.
- [18] B. Jacob, S. Kligys, B. Chen, M. Zhu, M. Tang, A. Howard, H. Adam, and D. Kalenichenko, “Quantization and training of neural networks for efficient integer-arithmetic-only inference,” in *Proceedings of the IEEE Conference on Computer Vision and Pattern Recognition*, pp. 2704–2713, 2018.
- [19] J. Yang, X. Shen, J. Xing, X. Tian, H. Li, B. Deng, J. Huang, and X.-s. Hua, “Quantization networks,” in *Proceedings of the IEEE Conference on Computer Vision and Pattern Recognition*, pp. 7308–7316, 2019.
- [20] D. Zhang, J. Yang, D. Ye, and G. Hua, “Lq-nets: Learned quantization for highly accurate and compact deep neural networks,” in *Proceedings of the European Conference on Computer Vision (ECCV)*, September 2018.
- [21] T. Sheng, C. Feng, S. Zhuo, X. Zhang, L. Shen, and M. Aleksic, “A quantization-friendly separable convolution for mobilenets,” in *2018 1st Workshop on Energy Efficient Machine Learning and Cognitive Computing for Embedded Applications (EMC2)*, pp. 14–18, IEEE, 2018.
- [22] J. Achterhold, J. M. Koehler, A. Schmeink, and T. Genewein, “Variational network quantization,” in *International Conference on Learning Representations*, 2018.
- [23] D. P. Kingma, T. Salimans, and M. Welling, “Variational dropout and the local reparameterization trick,” *arXiv preprint arXiv:1506.02557*, 2015. <https://arxiv.org/pdf/1506.02557.pdf>.
- [24] K. Neklyudov, D. Molchanov, A. Ashukha, and D. Vetrov, “Structured bayesian pruning via log-normal multiplicative noise,” *arXiv preprint arXiv:1705.07283*, 2017. <https://arxiv.org/pdf/1705.07283.pdf>.
- [25] M. Abadi, A. Agarwal, P. Barham, E. Brevdo, Z. Chen, C. Citro, G. S. Corrado, A. Davis, J. Dean, M. Devin, S. Ghemawat, I. Goodfellow, A. Harp, G. Irving, M. Isard, Y. Jia, R. Jozefowicz, L. Kaiser, M. Kudlur, J. Levenberg, D. Mané, R. Monga, S. Moore, D. Murray, C. Olah, M. Schuster, J. Shlens, B. Steiner, I. Sutskever, K. Talwar, P. Tucker, V. Vanhoucke, V. Vasudevan, F. Viégas, O. Vinyals, P. Warden, M. Wattenberg, M. Wicke, Y. Yu, and X. Zheng, “TensorFlow: Model optimization,” 2015. Software available from tensorflow.org.
- [26] A. Paszke, S. Gross, F. Massa, A. Lerer, J. Bradbury, G. Chanan, T. Killeen, Z. Lin, N. Gimelshein, L. Antiga, A. Desmaison, A. Kopf, E. Yang, Z. DeVito, M. Raison, A. Tejani, S. Chilamkurthy, B. Steiner, L. Fang, J. Bai, and S. Chintala, “Pytorch: Quantization,” in *Advances in Neural Information Processing Systems 32* (H. Wallach, H. Larochelle, A. Beygelzimer, F. d’Alché-Buc, E. Fox, and R. Garnett, eds.), pp. 8024–8035, Curran Associates, Inc., 2019.
- [27] H. Li, S. De, Z. Xu, C. Studer, H. Samet, and T. Goldstein, “Training quantized nets: A deeper understanding,” in *Proceedings of the 31st International Conference on Neural Information Processing Systems*, pp. 5813–5823, 2017.
- [28] D. Alistarh, D. Grubic, J. Li, R. Tomioka, and M. Vojnovic, “Qsgd: Communication-efficient sgd via gradient quantization and encoding,” *Advances in Neural Information Processing Systems*, vol. 30, pp. 1709–1720, 2017.
- [29] D. Alistarh, D. Grubic, J. Li, R. Tomioka, and M. Vojnovic, “Qsgd: Communication-efficient sgd via gradient quantization and encoding,” *arXiv preprint arXiv:1610.02132*, 2016. <https://arxiv.org/pdf/1610.02132.pdf>.
- [30] A. Rajagopal, D. A. Vink, S. I. Venieris, and C.-S. Bouganis, “Multi-precision policy enforced

- training (muppet): A precision-switching strategy for quantised fixed-point training of cnns,” *arXiv preprint arXiv:2006.09049*, 2020.
- [31] J. H. Wilkinson, *Rounding errors in algebraic processes*. Courier Corporation, 1994.
- [32] A. Paszke, S. Gross, F. Massa, A. Lerer, J. Bradbury, G. Chanan, T. Killeen, Z. Lin, N. Gimelshein, L. Antiga, A. Desmaison, A. Kopf, E. Yang, Z. DeVito, M. Raison, A. Tejani, S. Chilamkurthy, B. Steiner, L. Fang, J. Bai, and S. Chintala, “Pytorch: An imperative style, high-performance deep learning library,” in *Advances in Neural Information Processing Systems 32* (H. Wallach, H. Larochelle, A. Beygelzimer, F. d’Alché-Buc, E. Fox, and R. Garnett, eds.), pp. 8024–8035, Curran Associates, Inc., 2019.
- [33] M. Abadi, A. Agarwal, P. Barham, E. Brevdo, Z. Chen, C. Citro, G. S. Corrado, A. Davis, J. Dean, M. Devin, S. Ghemawat, I. Goodfellow, A. Harp, G. Irving, M. Isard, Y. Jia, R. Jozefowicz, L. Kaiser, M. Kudlur, J. Levenberg, D. Mané, R. Monga, S. Moore, D. Murray, C. Olah, M. Schuster, J. Shlens, B. Steiner, I. Sutskever, K. Talwar, P. Tucker, V. Vanhoucke, V. Vasudevan, F. Viégas, O. Vinyals, P. Warden, M. Wattenberg, M. Wicke, Y. Yu, and X. Zheng, “TensorFlow: Large-scale machine learning on heterogeneous systems,” 2015. Software available from tensorflow.org.
- [34] J. H. Wilkinson, *Rounding errors in algebraic processes*. Courier Corporation, 1994.
- [35] J. H. Wilkinson, *Rounding errors in algebraic processes*. Courier Corporation, 1994.
- [36] M. Hopkins, M. Mikaitis, D. R. Lester, and S. Furber, “Stochastic rounding and reduced-precision fixed-point arithmetic for solving neural ordinary differential equations,” *Philosophical Transactions of the Royal Society A*, vol. 378, no. 2166, p. 20190052, 2020.
- [37] D. Yin, A. Pananjady, M. Lam, D. Papailiopoulos, K. Ramchandran, and P. Bartlett, “Gradient diversity: a key ingredient for scalable distributed learning,” in *International Conference on Artificial Intelligence and Statistics*, pp. 1998–2007, 2018.
- [38] A. Kerr, H. Wu, M. Gupta, D. Blasig, P. Ramanani, N. Farooqui, P. Majcher, P. Springer, J. Wang, S. Yokim, M. Hohnerbach, A. Atluri, D. Tanner, T. Costa, J. Demouth, B. Fahs, M. Goldfarb, M. Hagog, F. Hu, A. Kaatz, T. Li, T. Liu, D. Merrill, K. Siu, M. Tavenrath, J. Tran, V. Wang, J. Wu, F. Xie, A. Xu, J. Yang, X. Zhang, N. Zhao, G. Bharambe, C. Cecka, L. Durant, O. Giroux, S. Jones, R. Kulkarni, B. Lebach, J. McCormack, and K. P. and, “Nvidia cutlass,” 2020. Online, accessed 15.07.2020.
- [39] D. P. Kingma and J. Ba, “Adam: A method for stochastic optimization,” *arXiv preprint arXiv:1412.6980*, 2014.
- [40] Y. LeCun, L. Bottou, Y. Bengio, and P. Haffner, “Gradient-based learning applied to document recognition,” *Proceedings of the IEEE*, vol. 86, no. 11, pp. 2278–2324, 1998.
- [41] L. Deng, “The mnist database of handwritten digit images for machine learning research [best of the web],” *IEEE Signal Processing Magazine*, vol. 29, no. 6, pp. 141–142, 2012.
- [42] G. H. Alex Krizhevsky, Vinod Nair, “The cifar-10 and cifar-100 dataset,” 2019. Online, accessed 15.07.2020.
- [43] X. Glorot and Y. Bengio, “Understanding the difficulty of training deep feedforward neural networks,” in *Proceedings of the thirteenth international conference on artificial intelligence and statistics*, pp. 249–256, 2010.
- [44] K. He, X. Zhang, S. Ren, and J. Sun, “Delving deep into rectifiers: Surpassing human-level performance on imagenet classification,” in *Proceedings of the IEEE international conference on computer vision*, pp. 1026–1034, 2015.

- [45] B. Hanin and D. Rolnick, “How to start training: The effect of initialization and architecture,” in *Advances in Neural Information Processing Systems*, pp. 571–581, 2018.
- [46] G. Klambauer, T. Unterthiner, A. Mayr, and S. Hochreiter, “Self-normalizing neural networks,” in *Advances in neural information processing systems*, pp. 971–980, 2017.
- [47] Y. A. LeCun, L. Bottou, G. B. Orr, and K.-R. Müller, “Efficient backprop,” in *Neural networks: Tricks of the trade*, pp. 9–48, Springer, 2012.
- [48] Y. Bhalgat, J. Lee, M. Nagel, T. Blankevoort, and N. Kwak, “Lsq+: Improving low-bit quantization through learnable offsets and better initialization,” in *Proceedings of the IEEE/CVF Conference on Computer Vision and Pattern Recognition Workshops*, pp. 696–697, 2020.
- [49] S. Basodi, C. Ji, H. Zhang, and Y. Pan, “Gradient amplification: An efficient way to train deep neural networks,” *arXiv preprint arXiv:2006.10560*, 2020. <https://arxiv.org/pdf/2006.10560.pdf>.
- [50] Z. Chen, V. Badrinarayanan, C.-Y. Lee, and A. Rabinovich, “Gradnorm: Gradient normalization for adaptive loss balancing in deep multitask networks,” in *International Conference on Machine Learning*, pp. 794–803, 2018.
- [51] T. Salimans and D. P. Kingma, “Weight normalization: A simple reparameterization to accelerate training of deep neural networks,” in *Advances in neural information processing systems*, pp. 901–909, 2016.
- [52] P. Zhou, J. Feng, C. Ma, C. Xiong, S. C. H. Hoi, and W. E, “Towards theoretically understanding why sgd generalizes better than adam in deep learning,” in *Advances in Neural Information Processing Systems* (H. Larochelle, M. Ranzato, R. Hadsell, M. F. Balcan, and H. Lin, eds.), vol. 33, pp. 21285–21296, Curran Associates, Inc., 2020.
- [53] P. M. Williams, “Bayesian regularization and pruning using a laplace prior,” *Neural computation*, vol. 7, no. 1, pp. 117–143, 1995.
- [54] A. Y. Ng, “Feature selection,  $l_1$  vs.  $l_2$  regularization, and rotational invariance,” in *Proceedings of the twenty-first international conference on Machine learning*, p. 78, 2004.
- [55] R. Tibshirani, “Regression shrinkage and selection via the lasso,” *Journal of the Royal Statistical Society: Series B (Methodological)*, vol. 58, no. 1, pp. 267–288, 1996.
- [56] H. Zou and T. Hastie, “Regularization and variable selection via the elastic net,” *Journal of the royal statistical society: series B (statistical methodology)*, vol. 67, no. 2, pp. 301–320, 2005.
- [57] N. Corporation, “NVIDIA DGX-1essential instrument for ai research,” 2017. Online, accessed 07.07.2021.